THADA fusion is a mechanism of IGF2BP3 activation and IGF1R signaling in thyroid cancer

Federica Panebianco[a,1], Lindsey M. Kelly[a,1], Pengyuan Liu[b], Shan Zhong[a], Sanja Dacic[a], Xiaosong Wang[a], Aatur D. Singhi[a], Rajiv Dhir[a], Simion I. Chiosea[a], Shih-Fan Kuan[a], Rohit Bhargava[a], David Dabbs[a], Sumita Trivedi[c], Manoj Gandhi[d], Rachel Diaz[d], Abigail I. Wald[a], Sally E. Carty[e], Robert L. Ferris[c], Adrian V. Lee[f], Marina N. Nikiforova[a], and Yuri E. Nikiforov[a,2]

[a]Department of Pathology and Laboratory Medicine, University of Pittsburgh School of Medicine, Pittsburgh, PA 15213; [b]Sir Run Run Shaw Hospital, School of Medicine, Zhejiang University, Hangzhou, Zhejiang 310058, China; [c]Department of Otolaryngology, University of Pittsburgh School of Medicine, Pittsburgh, PA 15213; [d]Affymetrix, Inc., Santa Clara, CA 95051; [e]Division of Endocrine Surgery, University of Pittsburgh School of Medicine, Pittsburgh, PA 15213; and [f]Department of Pharmacology and Chemical Biology, Women's Cancer Research Center, University of Pittsburgh Cancer Institute, Pittsburgh, PA 15213

Edited by Albert de la Chapelle, Ohio State University Comprehensive Cancer Center, Columbus, OH, and approved January 17, 2017 (received for review September 19, 2016)

Thyroid cancer development is driven by known point mutations or gene fusions found in ∼90% of cases, whereas driver mutations in the remaining tumors are unknown. The insulin-like growth factor 2 mRNA-binding protein 3 (IGF2BP3) plays an important role in cancer, yet the mechanisms of its activation in cancer cells remain poorly understood. Using whole-transcriptome and whole-genome analyses, we identified a recurrent fusion between the thyroid adenoma-associated (*THADA*) gene on chromosome 2 and the *LOC389473* gene on chromosome 7 located 12 kb upstream of the *IGF2BP3* gene. We show that *THADA* fusion to *LOC389473* and other regions in the vicinity does not result in the formation of a chimeric protein but instead leads to strong overexpression of the full-length IGF2BP3 mRNA and protein, increased IGF2 translation and IGF1 receptor (IGF1R) signaling via PI3K and MAPK cascades, and promotion of cell proliferation, invasion, and transformation. *THADA* fusions and IGF2BP3 overexpression are found in ∼5% of thyroid cancers that lack any other driver mutations. We also find that strong IGF2BP3 overexpression via gene fusion, amplification, or other mechanisms occurs in 5 to 15% of several other cancer types. Finally, we provide in vitro and in vivo evidence that growth of IGF2BP3-driven cells and tumors may be blocked by IGF1R inhibition, raising the possibility that IGF2BP3 overexpression in cancer cells may predict an anti-IGF1R benefit.

thyroid cancer | genetics | chromosomal rearrangements | IGF2BP3 | IGF1R

Genome-wide sequencing analyses offer a valuable tool for better understanding of genetic mechanisms of tumorigenesis and identifying new therapeutic targets for cancer. Such approaches have led to identification of driver mutations in the majority of thyroid cancer cases (1, 2). They confirmed that point mutations and gene fusions leading to the activation of the MAPK and PI3K/AKT signaling pathways are crucial for tumorigenesis and progression of these tumors. Among papillary thyroid carcinomas (PTCs), the most common type of thyroid cancer, ∼75% of tumors have driver point mutations, whereas ∼15% show nonoverlapping chromosomal rearrangements typically leading to the activation of receptor tyrosine kinases (1). Driver point mutations or gene fusions in the remaining PTCs remain unknown.

Typically, oncogenic chromosomal rearrangements result in an in-frame fusion of a 5′ portion of an actively transcribed gene to a functionally important 3′ portion of an oncogene, frequently coding for the kinase domain, leading to gene expression and constitutive kinase activation (3). Other, less common mechanisms include translocation of an oncogene to a region of actively transcribed chromatin, leading to gene activation without formation of the chimeric gene products (4–6). Such events are more difficult to identify as biologically relevant during the analysis of next-generation sequencing data, because no typical in-frame fusion of two coding gene sequences can be found. This may be responsible for a failure to identify driver gene fusions in a significant proportion of common cancers with currently unknown driver mutations (7).

In this study, we used whole-transcriptome (RNA sequencing; RNA-seq) and whole-genome sequencing (WGS) of PTCs to identify recurrent fusions between the thyroid adenoma-associated (*THADA*) gene on chromosome 2 and a genomic region on chromosome 7 and demonstrate that it does not lead to the formation of the chimeric protein but instead results in strong overexpression of the downstream insulin-like growth factor 2 mRNA-binding protein 3 (*IGF2BP3*) gene, which is a transforming event in thyroid tumors and a potential therapeutic target for IGF1 receptor (IGF1R) inhibitors in different cancer types.

Results

Identification of *THADA–LOC389473* and *THADA–IGF2BP3* Fusions. To identify novel driver events in thyroid cancer, a prescreened group of 25 PTCs lacking all known mutations was studied by RNA-seq (21 tumors) or WGS (4 tumors) using paired-end sequencing on an Illumina HiSeq system. Using RNA-seq, six tumors were found to have gene fusions involving the *THADA* gene located on 2p21. In four tumors (T1, T2, T3, and T5), RNA-seq results revealed

Significance

Thyroid cancer is the fastest-growing cancer type in the United States, yet its molecular mechanisms are not fully understood. Here we report the identification and characterization of a gene fusion involving the thyroid adenoma-associated (*THADA*) and *LOC389473* genes in papillary thyroid cancers, which leads to strong overexpression of insulin-like growth factor 2 mRNA-binding protein 3 (IGF2BP3) and signaling via the IGF2/IGF1 receptor (IGF1R) pathway. As a result, we report a previously unknown structural mechanism responsible for IGF2BP3 overexpression in cancer. We also show that IGF2BP3 overexpression via different mechanisms can be found in 5 to 15% of several cancer types, and demonstrate that growth of these tumors can be blocked by IGF1R inhibitors. This raises the possibility that IGF2BP3 overexpression may be used to predict therapeutic response to IGF1R inhibition in cancer cells.

Author contributions: F.P., L.M.K., S.E.C., R.L.F., A.V.L., M.N.N., and Y.E.N. designed research; F.P., L.M.K., S.D., R. Dhir, S.T., M.G., R. Diaz, A.I.W., S.E.C., R.L.F., A.V.L., M.N.N., and Y.E.N. performed research; F.P., L.M.K., P.L., S.Z., S.D., X.W., A.D.S., R. Dhir, S.I.C., S.-F.K., R.B., D.D., M.G., R. Diaz, A.I.W., S.E.C., R.L.F., A.V.L., M.N.N., and Y.E.N. analyzed data; and F.P., L.M.K., M.G., and Y.E.N. wrote the paper.

Conflict of interest statement: Y.E.N. is a consultant for Quest Diagnostics.

This article is a PNAS Direct Submission.

[1]F.P. and L.M.K. contributed equally to this work.

[2]To whom correspondence should be addressed. Email: nikiforovye@upmc.edu.

This article contains supporting information online at www.pnas.org/lookup/suppl/doi:10.1073/pnas.1614265114/-/DCSupplemental.

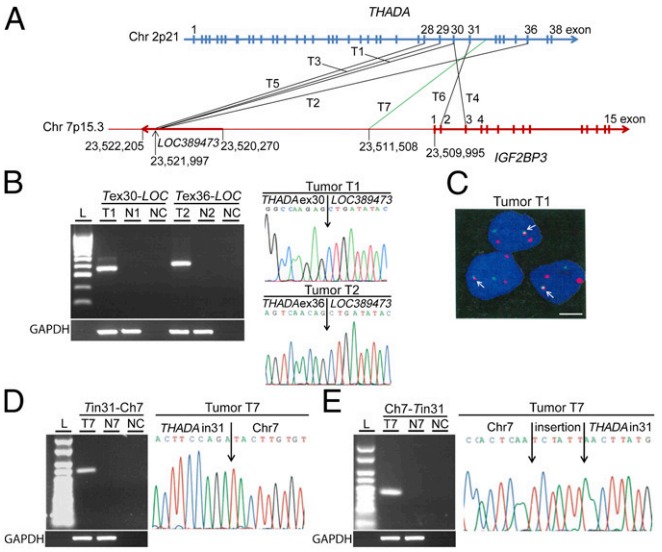

Fig. 1. Discovery and confirmation of *THADA* gene fusions. (*A*) Scheme of gene fusions identified in six thyroid cancers (T1 to T6) on the mRNA level by RNA-seq (black lines) and in one tumor (T7) on the DNA level by WGS (green line). Chromosome positions are based on Genome Reference Consortium, build 37 (GRCh37)/UCSC (genome browser hosted by the University of California, Santa Cruz) version 19 (hg19). (*B*) Confirmation of the *THADA–LOC389473* fusion in tumors T1 and T2 by RT-PCR and Sanger sequencing (remaining tumors are shown in *SI Appendix*, Fig. S1). (*C*) Confirmation of a fusion between *THADA* and a locus located upstream of *IGF2BP3* in T1 by FISH with probes for *THADA* (red) and *IGF2BP3* (green). All tumor cells show a pair of fused red and green signals (arrows) (other tumors are shown in *SI Appendix*, Fig. S3). (Scale bar, 5 μm.) (*D*) Confirmation of the fusion between *THADA* and a region 1.5 kb upstream of the *IGF2BP3* gene identified by WGS using PCR and Sanger sequencing. (*E*) Detection of a predicted reciprocal fusion between a region 1.5 kb upstream of *IGF2BP3* and *THADA*. *GAPDH* amplification was used as a control for RNA integrity and is shown in both *D* and *E*. (Ch7, Ch7 23,511,508; ex, exon; *I*, *IGF2BP3*; in, intron; L, ladder; *LOC*, *LOC38947*; N, normal tissue; NC, negative control; *T*, *THADA*.)

fusions between different exons (28, 29, 30, or 36) of *THADA* and the noncoding region on 7p15.3 [chromosome (chr.) position 23,521,997] (Fig. 1*A* and *SI Appendix*, Table S1). This region is located 12 kb upstream of the *IGF2BP3* gene and appears to contain a putative *Homo sapiens* gene, *LOC389473*. RNA-seq analysis of the other two tumors revealed fusions between exon 30 of *THADA* and exon 3 of *IGF2BP3* (T4) or between exon 31 of *THADA* and exon 2 of *IGF2BP3* (T6). All fusions were confirmed by RT-PCR and Sanger sequencing (Fig. 1*B* and *SI Appendix*, Fig. S1). In addition, upon manual inspection of RNA-seq reads for T4 with the *THADA* exon 30-to-*IGF2BP3* exon 3 fusion, single reads spanning *THADA* exon 30 and *LOC389473* were also identified and confirmed by RT-PCR and Sanger sequencing (*SI Appendix*, Fig. S1). Using WGS, one additional tumor (T7) was found to have a fusion between intron 31 of *THADA* and a region located 1.5 kb upstream of the *IGF2BP3* gene (chr. position 23,511,508) (Fig. 1*A*). The fusion was confirmed by PCR and Sanger sequencing of tumor DNA (Fig. 1*D*), and a reciprocal fusion was detected (Fig. 1*E*), indicating that it is a result of a balanced translocation between chromosomes 2 and 7. However, no chimeric mRNA involving *THADA* exon 31 fused with any of the first four *IGF2BP3* exons was detected by RT-PCR (*SI Appendix*, Fig. S2). The *t*(2;7) rearrangement was further confirmed by FISH in each of the five tumors studied (Fig. 1*C* and *SI Appendix*, Fig. S3).

***THADA–LOC389473* Results in Overexpression of Downstream *IGF2BP3*.** The *THADA–LOC389473* fusion places the partner genes in a head-to-tail orientation and they transcribe in opposite directions, so the fusion mRNA contains a stop codon downstream of the fusion point in all four tumors (*SI Appendix*, Fig. S4), suggesting that *THADA–LOC389473* is unlikely to yield a functional protein. This, together with finding the *THADA–IGF2BP3* fusions in other tumors, allowed us to hypothesize that *THADA–LOC389473* may affect carcinogenesis instead via altering the *IGF2BP3* gene. To test this, we first detected the expression levels of *THADA* and *IGF2BP3* in normal thyroid tissues and tumors by quantitative (q)RT-PCR. The analysis showed that *THADA* was expressed at a high level in normal thyroid follicular cells compared with other cell types studied, and its expression was not altered in thyroid cancers positive or negative for *THADA* fusions (Fig. 2*A* and *SI Appendix*, Fig. S5). In contrast, *IGF2BP3* was found to be expressed at a very low level in normal thyroid cells and tumors negative for the fusion, but its expression was increased 90- to 102-fold in all tumors carrying the fusion (Fig. 2*B*). Similar findings were observed in the RNA-seq data, which showed the increased expression of the full-length *IGF2BP3* mRNA in tumors positive for *THADA–LOC389473* and *THADA–IGF2BP3* fusions (Fig. 2*C* and *SI Appendix*, Fig. S5). Similarly, by Western blot analysis, all six tumors studied showed high levels of IGF2BP3 protein of ∼69-kDa molecular weight, corresponding to a full-length protein, and no other protein products that would correspond to a chimeric gene product (Fig. 2*D*). The analysis included tumors with *THADA–LOC389473* and *THADA–IGF2BP3* fusions and a *THADA* intron fused to a sequence 1.5 kb upstream of *IGF2BP3*. Further, immunohistochemical analysis with IGF2BP3 antibody showed strong cytoplasmic immunoreactivity in all studied fusion-positive tumors but not in adjacent normal thyroid tissue (Fig. 2*E*). These data indicate that fusion between the *THADA* gene and *LOC389473*, a predicted gene located 12 kb upstream of the *IGF2BP3* gene, is unlikely to produce a functional chimeric gene but instead results in strong overexpression of the full-length *IGF2BP3* transcript and

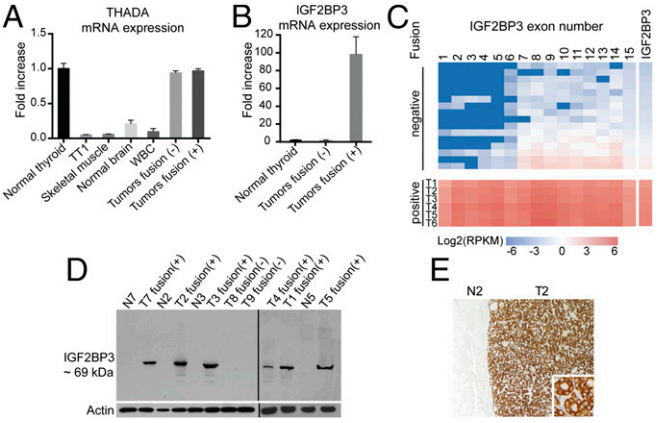

Fig. 2. Effect of *THADA* gene fusions on IGF2BP3 expression. (*A*) Expression levels (mean ± SD) of THADA mRNA detected by qRT-PCR in different indicated normal tissues ($n = 4$ for each tissue type), thyroid C cell-derived tumor cell line TT1, and thyroid tumors negative ($n = 6$) and positive ($n = 6$) for *THADA* fusions (tumors T1, T2, and T4 to T7). (*B*) Expression levels (mean ± SD) of *IGF2BP3* mRNA in normal thyroid tissue ($n = 4$) and tumors negative ($n = 6$) and positive ($n = 6$) for THADA fusions as detected by qRT-PCR. (*C*) mRNA expression levels of each exon and the full *IGF2BP3* gene showing overexpression of the full-length IGF2BP3 in samples positive (+) for *THADA–LOC389473* (tumors T1 to T3 and T5) or *THADA–IGF2BP3* (tumors T4 and T6) compared with samples negative (–) for fusions. Each box represents an exon, and the boxes are colored according to the logarithm of their expression levels as measured in RPKMs (reads per kilobase per million reads). (*D*) Western blot analysis of thyroid tumors (T) positive (+) and negative (–) for fusions and the corresponding normal tissues (N). The analysis included four tumors with *THADA–LOC389473* fusions (T1 to T3 and T5), a tumor with *THADA* exon30–*IGF2BP3* exon3 fusion (T4), and a tumor with *THADA* intron 31 fused to 1.5 kb upstream of *IGF2BP3* (T7). (*E*) Representative immunostaining of T2 positive for *THADA–LOC389473* showing strong cytoplasmic immunoreactivity with anti-IGF2BP3 antibody in the tumor (T2) and a complete lack of staining of normal thyroid tissue (N2). (Magnification: ×100; *Inset*, ×400.)

protein, likely due to juxtaposition of the *IGF2BP3* chromosomal locus on 7p15.3 to the actively transcribed *THADA* locus on 2p21.

Overexpression of IGF2BP3 Leads to an Increase in IGF2 Protein and Activation of the PI3K and MAPK Pathways. IGF2BP3 is known to serve as a translational activator of *IGF2* mRNA. Therefore, we determined the expression of IGF2 mRNA and protein in thyroid tumors positive and negative for *THADA* fusions. Using qRT-PCR, no difference in IGF2 mRNA levels was detected (Fig. 3*A*). This was confirmed by RNA in situ hybridization (ISH), which showed low levels of *IGF2* mRNA in the fusion-positive tumors, similar to those seen in adjacent normal thyroid tissue, in contrast to the high levels of IGF2BP3 mRNA in the fusion-positive tumors (Fig. 3*B*). However, using Western blotting, a significant increase in IGF2 protein was found in all tested tumors positive for the fusion and IGF2BP3 overexpression (Fig. 3*C*).

IGF2 is known to act as an autocrine and paracrine regulator of IGF1R (8, 9), leading to activation of the PI3K and MAPK signaling pathways (9, 10). Therefore, we examined whether the increase in IGF2 protein in these human tumor tissues was associated with the increased phosphorylation of AKT and ERK proteins. Using Western blot analysis, we showed increased pAKT and pERK in all tumors positive for the fusion (Fig. 3*C*). The effect of IGF2BP3 overexpression on IGF2 signaling was further confirmed in vitro. Overexpression of IGF2BP3 in HEK293 cells led to an increase in IGF2 protein, but not mRNA, and increased phosphorylation of AKT and ERK proteins (Fig. 3 *D* and *E*). The knockdown experiments were performed in PaCa-2 pancreatic cancer cells, which have a very high level of IGF2BP3 expression, based on the reference database for gene expression analysis (Laboratory for Systems Biology and Medicine) (www.lsbm.org/site_e/database/index.html), which we confirmed by Western blot and immunohistochemistry (IHC) (Fig. 3 *F* and *H*). Knockdown of *IGF2BP3* using siRNA led to a significant reduction in IGF2 protein levels and decreased pAKT and pERK (Fig. 3 *G* and *H*), confirming the impact of IGF2BP3 on translational activation of IGF2 and its downstream signaling.

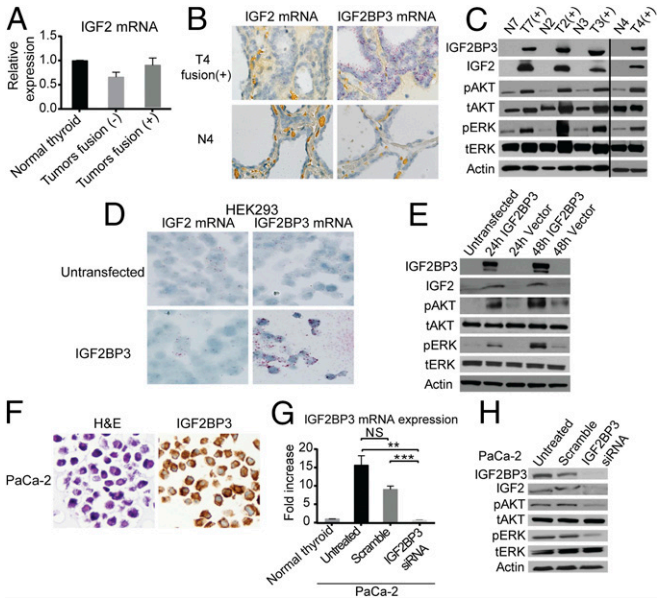

Fig. 3. Overexpression of IGF2BP3 leads to an increase in IGF2 and activation of downstream signaling. (*A*) Expression levels (mean ± SD) of IGF2 mRNA in normal thyroid tissues ($n = 4$) and tumors negative ($n = 5$) and positive ($n = 5$) for *THADA* fusions (T1, T2, T4, and T7). (*B*) Representative RNA ISH images showing low levels of IGF2 mRNA in fusion-positive tumors and adjacent normal thyroid tissue but high levels of IGF2BP3 mRNA in fusion-positive tumors compared with adjacent normal thyroid. (*C*) Western blot analysis of protein lysates of fusion-positive tumors (T2 to T4 and T7) and normal thyroid with the indicated antibodies. (*D*) Representative RNA ISH stains for IGF2 and IGF2BP3 of HEK293 cells before and after transfection with IGF2BP3 expression vector. (*E*) Western blot analysis of protein lysates of HEK293 cells before and after transfection with IGF2BP3 expression vector. (*F*) Morphology (hematoxylin and eosin stain; H&E) and immunohistochemistry with anti-IGF2BP3 antibody showing strong cytoplasmic immunoreactivity in PaCa-2 cells. (*G*) qRT-PCR analysis of IGF2BP3 mRNA levels in PaCa-2 cells, untreated and transfected with IGF2BP3 siRNAs or scramble control. Data from experiments repeated in quadruplicate are shown as mean ± SD (NS, difference not significant; $^{**}P < 0.01$, $^{***}P < 0.001$; two-tailed Student's *t* test). (*H*) Western blot analysis of protein lysates of PaCa-2 cells, untreated and 48 h after IGF2BP3 knockdown by siRNA. (Magnification: *B*, 100×; *D* and *F*, 400×.)

IGF2BP3 Overexpression Drives Cell Proliferation, Invasion, and Transformation. To study the biological effect of *THADA* fusions and IGF2BP3 overexpression in thyroid and other cell types, full-length *IGF2BP3* mRNA was overexpressed in FTC133, HEK293, and U2OS cells, all with low levels of endogenous expression of IGF2BP3. Overexpression of IGF2BP3 resulted in a significant increase in proliferation in all three cell lines (Fig. 4 *A*–*C*). In a reverse experiment, silencing of IGF2BP3 in PaCa-2 cancer cells, which have high levels of IGF2BP3 expression, led to a significantly reduced growth rate (Fig. 4*D*).

Next, we explored the impact of IGF2BP3 overexpression on cell migration and invasion. Using a wound-healing assay, IGF2BP3 overexpression in HEK293 cells led to a significantly faster migration (Fig. 4*E*), whereas IGF2BP3 knockdown in PaCa-2 cells resulted in decreased cell migration (Fig. 4*F*). Similarly, a Matrigel invasion assay showed that overexpression of IGF2BP3 in HEK293 cells led to a significant enhancement of cell invasion, and knockdown of IGF2BP3 in PaCa-2 cells resulted in reduced cell invasiveness (Fig. 4 *G* and *H*).

Finally, we studied the impact of IGF2BP3 overexpression on cell transformation. Using a soft-agar colony-formation assay, FTC133 thyroid cells transfected with IGF2BP3 vector showed a significant increase in colony formation in the soft agar compared with empty vector (Fig. 4*I*), indicating enhanced anchorage-independent growth, a characteristic of transformed cells. In a reverse experiment, knockdown of IGF2BP3 expression in PaCa-2 cancer cells resulted in a significant reduction of colony formation in soft agar (Fig. 4*J*). Together, these data indicate that IGF2BP3 overexpression promotes cell proliferation, migration, invasion, and transformation in thyroid and other cell types.

Frequency of IGF2BP3 Overexpression via Gene Fusion and Other Mechanisms in Thyroid and Other Cancers. To evaluate the rate of IGF2BP3 alterations in thyroid and other tumors, we first developed an IHC assay for specific and sensitive detection of overexpression of IGF2BP3 protein in tumors carrying *THADA–LOC389473* and *THADA–IGF2BP3* fusions. For this, IHC for IGF2BP3 was titrated using 7 fusion-positive and 18 fusion-negative thyroid cancers to achieve strong and diffuse cytoplasmic immunoreactivity in all positive cancers and complete absence of immunoreactivity in fusion-negative cancers (*SI Appendix*, Fig. S6*A*). Further, a targeted next-generation sequencing (NGS) was used for quantitative assessment of IGF2BP3 mRNA. Analysis of 192 PTCs, which represented a series of consecutive tumors with this diagnosis analyzed by targeted NGS, revealed 10 (5.2%) cases with strong IGF2BP3 immunoreactivity; all were confirmed to have high levels of IGF2BP3 mRNA expression (*SI Appendix*, Fig. S6*B*). Using RT-PCR, 9 out of the 10 (90%) tumors were positive for a fusion, typically *THADA–LOC389473*. Rearrangement involving the *IGF2BP3* region was further confirmed by FISH in all 10 IHC-positive thyroid cancers (*SI Appendix*, Fig. S6*C*). This demonstrated high specificity of the IHC assay in detecting tumors with IGF2BP3 overexpression caused by chromosomal rearrangements. It also showed that chromosomal rearrangement involving *THADA* fused to a chromosomal region upstream of *IGF2BP3* is a dominant mechanism of IGF2BP3 overexpression in PTC.

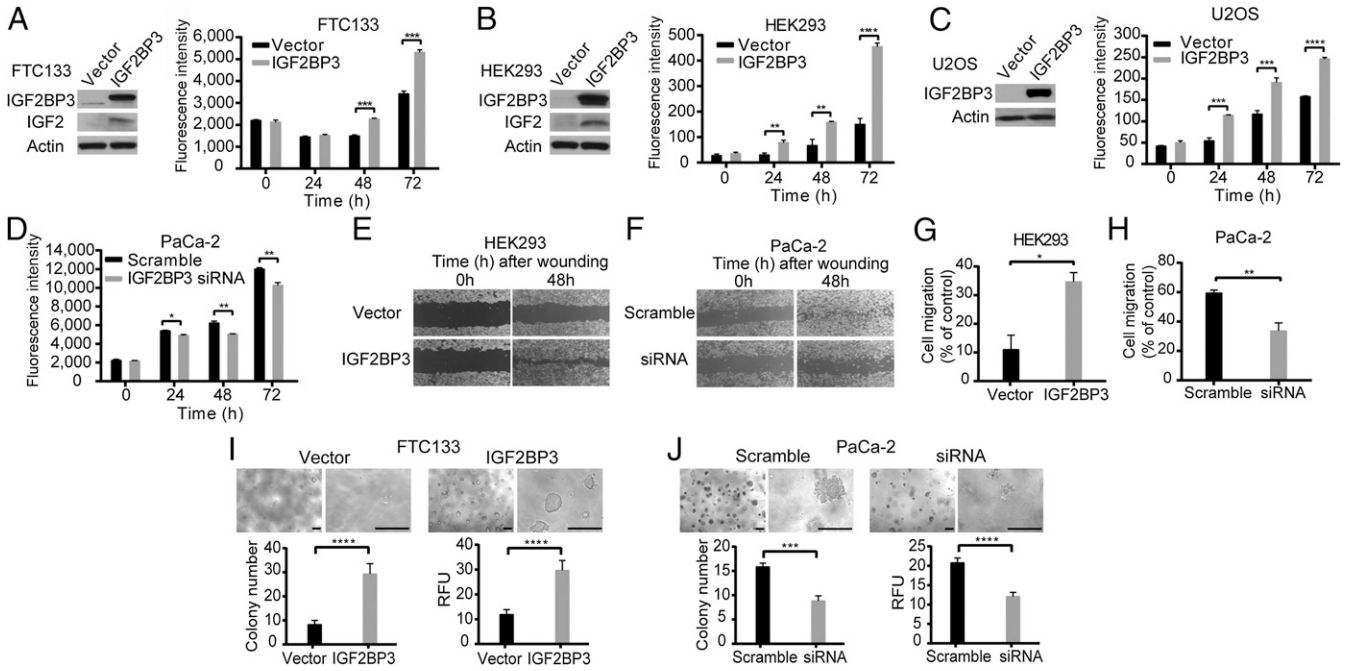

Fig. 4. Biological effects of IGF2BP3 overexpression in vitro. (*A–C*) Overexpression of IGF2BP3 confirmed by Western blot analyses 24 h posttransfection in FTC133 (*A*), HEK293 (*B*), and U2OS (*C*) cells resulted in increased cell proliferation in each cell type. Data from experiments repeated in quadruplicate are shown as mean ± SD (**$P < 0.01$, ***$P < 0.001$, ****$P < 0.0001$; two-tailed Student's *t* test). (*D*) siRNA knockdown of IGF2BP3 expression in PaCa-2 pancreatic cancer cells with high levels of IGF2BP3 expression led to decreased cell proliferation (*$P < 0.05$, **$P < 0.01$; two-tailed Student's *t* test). (*E* and *F*) Wound-healing assay repeated in triplicate. (*E*) Overexpression of IGF2BP3 in HEK293 cells showed increased cell migration and wound healing. (*F*) Knockdown of IGF2BP3 by siRNA in PaCa-2 cells resulted in inhibition of cell migration and slower wound healing. (*G* and *H*) Matrigel cell-invasion assay; data from experiments repeated in quadruplicate are shown as mean ± SD (*$P < 0.05$, **$P < 0.01$; two-tailed Student's *t* test). (*G*) HEK293 cells transfected with IGF2BP3 or empty vector. (*H*) PaCa-2 cells after knockdown of IGF2BP3 by siRNA. (*I* and *J*) Soft-agar colony-formation assay of (*I*) FTC133 cells transfected with empty vector or IGF2BP3 and (*J*) PaCa-2 cells transfected with scramble or IGF2BP3 siRNA after 7 d in culture. Shown are representative areas at 50× and 200× magnification (*Top*) and quantitative analysis of colony formation (*Bottom*). (Scale bars, 200 μm.) Number of colonies containing >50 cells counted under the microscope (*Left*) and using the fluorescence-based CytoSelect Cell Transformation Assay Kit (*Right*). Data from experiments repeated in quadruplicate are shown as mean ± SD (***$P < 0.001$, ****$P < 0.0001$; two-tailed Student's *t* test).

Next, we studied clinical and phenotypic features of thyroid cancers that showed IGF2BP3 overexpression. These tumors were characterized by slight female predominance (1.5:1), mean patient age of 48.9 y, and tumor size ranging from 1.6 to 9 cm (mean 3.8 cm). Despite the large tumor size, microscopically the tumors were either encapsulated ($n = 5$) or well-circumscribed ($n = 5$), with the follicular growth pattern characteristic of the follicular variant of PTC or noninvasive follicular thyroid tumor with papillary-like nuclear features (NIFTPs) (11) (*SI Appendix*, Fig. S6*D*). None of them showed other common driver mutations known to occur in thyroid cancer (e.g., *BRAF*, *RAS*), providing additional evidence for *THADA–LOC389473* and *THADA–IGF2BP3* fusions being a driver event in these tumors.

Further, we assessed the frequency of IGF2BP3 overexpression and its mechanisms in other cancer types. Using the IGF2BP3 IHC assay to screen tissue microarrays of 12 common cancer types, we found strong and diffuse immunoreactivity in 14.2% of pancreatic cancers, 12.6% of lung squamous cell carcinomas, 10.1% of lung adenocarcinomas, 10% of gastric cancers, 9.7% of cholangiocarcinomas, 9.1% of bladder cancers, 7.5% of ovarian cancers, and 3.8% of colon cancers (*SI Appendix*, Fig. S6 *E* and *F* and Table S2). Using FISH analysis of selected IHC-positive cancers, chromosomal rearrangements involving the *IGF2BP3* region were identified in 3/12 (25%) pancreatobiliary cancers (*SI Appendix*, Fig. S6 *F* and *G*), and *IGF2BP3* amplification in 3/18 (16.7%) IHC-positive lung adenocarcinomas, 1/8 (12.5%) pancreatic, and 1/5 (20%) bladder cancers (*SI Appendix*, Fig. S6 *F* and *H* and Table S2). These findings are in agreement with the cancer genome atlas (TCGA) data, where amplification of *IGF2BP3* was found in 0 to 7.1% of different cancer types (*SI Appendix*, Table S3). This suggests that in addition to gene fusions, many nonthyroid cancers have IGF2BP3 overexpression, which is likely due to gene amplifications or other, possibly epigenetic, mechanisms such as aberrant methylation (*SI Appendix*, Fig. S6*I*). Overall, these data demonstrate that strong overexpression of IGF2BP3, driven by gene fusions as well as other genetic and possibly epigenetic mechanisms, occurs in a distinct subset of thyroid and other cancer types.

Effects of IGF1R Inhibition on Growth of Cancer Cells Overexpressing IGF2BP3. The data presented above indicate that IGF2BP3 overexpression via chromosomal rearrangement and other mechanisms occurs in a distinct subset of thyroid and other cancers and results in an increase in IGF2 protein, signaling via IGF1R, and cell proliferation, invasion, and transformation. Increased IGF1R signaling has been linked to elevated cancer risk and more aggressive behavior of different cancers, and pharmacological inhibitors of IGF1R, such as the small-molecule inhibitor OSI-906 (Linsitinib), are available (12, 13). Therefore, we tested the effects of IGF1R inhibition on the growth of cancer cells driven by IGF2BP3 overexpression. First, we studied whether activation of the AKT and MAPK pathways and cell growth induced by IGF2BP3 overexpression are affected by inhibiting IGF1R by OSI-906 in vitro. Western blotting showed that inhibition of IGF1R blocked phosphorylation of AKT, S6, and ERK induced by IGF2BP3 overexpression in HEK293 cells (Fig. 5*A*). Further, we found that inhibition of IGF1R by OSI-906 led to dose-dependent growth inhibition of PaCa-2 cancer cells, which strongly overexpress IGF2BP3, but did not have any effects on FTC133 and U2OS cells with low levels of IGF2BP3 expression (Fig. 5*B*). However, when IGF2BP3 expression was induced in FTC133 and U2OS cells by transient transfection, both cell types

acquired sensitivity to growth inhibition by OSI-906, and subsequent inhibition of IGF1R returned the cells to an IGF2BP3-negative–like state (Fig. 5*C*). Similar effects of IGF1R inhibition were observed on migration and invasion of PaCa-2 cells (Fig. 5 *D* and *E*). Further, OSI-906 treatment of PaCa-2 cells led to significant reduction of colony formation in soft agar (Fig. 5*F*).

To determine whether the inhibitory effect of OSI-906 on cell proliferation is mediated by IGF2, we tested whether the inhibition of PaCa-2 cell proliferation following IGF2BP3 knockdown can be rescued by IGF2. Indeed, the reduction in PaCa-2 cell growth by IGF2BP3 siRNA was reversed after supplementing the cell-culture medium with sufficient concentrations of exogenous IGF2 (Fig. 5*G*).

Next, we explored whether growth of tumor cells overexpressing IGF2BP3 can be blocked via IGF1R inhibition in vivo. We used the pancreatic cancer cells PaCa-2 and colon cancer cells Caco-2, both expressing IGF2BP3 at high levels (Fig. 5*B*), and the thyroid cancer cells FTC133, with low levels of IGF2BP3 expression, to establish tumors growing in nude mice at the sites of s.c. cell injection. Treatment of mice with therapeutic doses of OSI-906 arrested growth of tumors originating from PaCa-2 and Caco-2 cells (Fig. 5*H*) but had no effect on the growth of FTC133-derived tumors (Fig. 5*I*). As expected, the inhibitory effect on tumor growth coincided with the reduction of phosphorylated IGF1R, AKT, S6, and ERK in the tumor tissue (Fig. 5*H*), whereas tumors originating from FTC133 and lacking IGF2BP3 expression did not show reduction in the phosphorylation of these proteins (Fig. 5*I*). These data show that growth of cancer cells overexpressing IGF2BP3 can be arrested by IGF1R inhibitors in vitro and in vivo, providing early evidence for a possible benefit of anti-IGF1R therapy in cancers with strong overexpression of IGF2BP3 induced by *THADA–LOC389473* fusion or other mechanisms.

Discussion

In this study, we report the discovery and characterization of a recurrent driver event in papillary thyroid cancer. The mutational landscape of this tumor is dominated by point mutations and gene fusions typically affecting genes coding for receptor tyrosine kinases (RTKs) or intracellular effectors propagating signals from RTKs via the MAPK and PI3K pathways (1). Here we report a different class of mutations that indirectly affect the expression of *IGF2BP3*, a gene coding for the IGF2 mRNA-binding protein that acts as a posttranscriptional regulator of IGF2 and via stimulation of the IGF1 receptor leads to the same end points, namely activation of MAPK and PI3K signaling. The

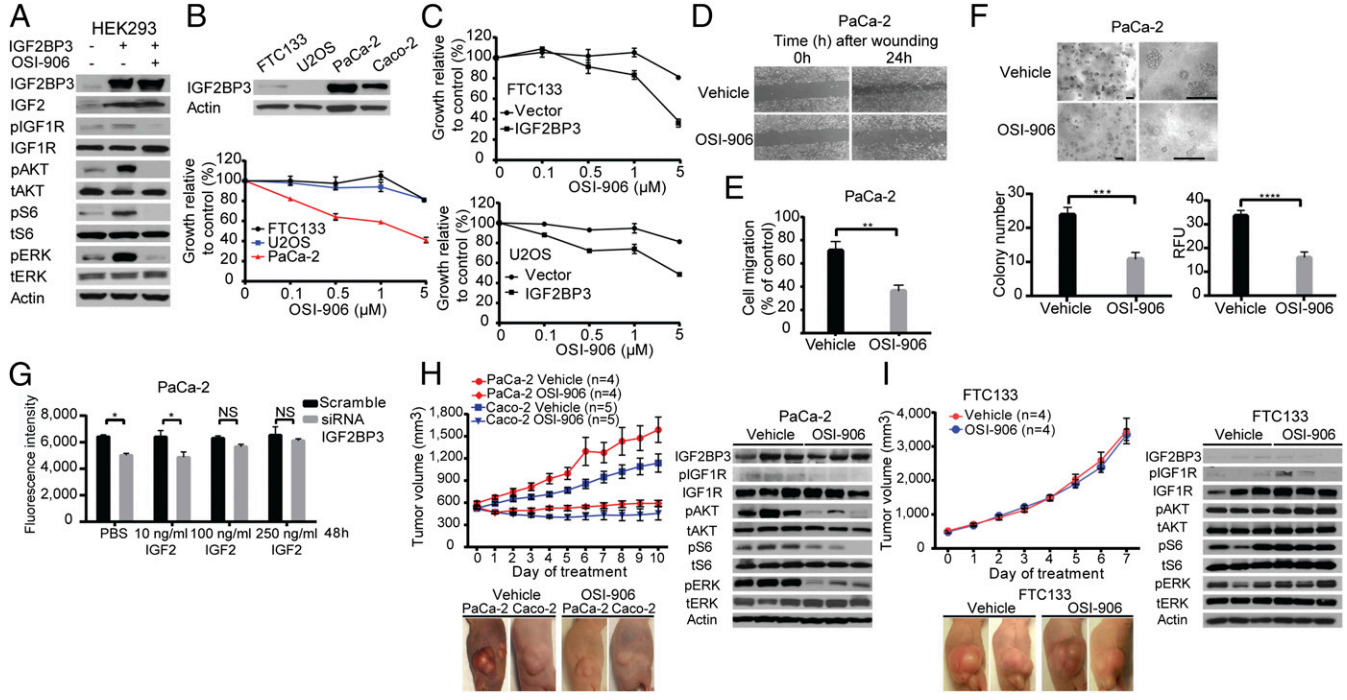

Fig. 5. Effects of IGF1R inhibition on the growth of cancer cells overexpressing IGF2BP3. (*A*) Western blot analysis showing that treatment with 5 μM IGF1R inhibitor (OSI-906) for 30 min led to the inhibition of IGF1R phosphorylation and downstream signaling in HEK293 cells induced by IGF2BP3. (*B*, *Top*) Western blot analysis of IGF2BP3 expression in FTC133, U2OS, PaCa-2, and Caco-2 cells. (*B*, *Bottom*) Treatment of the indicated cells with OSI-906 for 72 h resulted in inhibition of proliferation of PaCa-2 cells expressing IGF2BP3 at high levels but no effect on the proliferation of FTC133 and U2OS cells, which lack IGF2BP3 expression. Data from the experiments repeated in quadruplicate were calculated as the percentage of viable cells after treatment with OSI-906 and are shown as mean ± SD. (*C*) Following the transfection of FTC133 and U2OS cells with IGF2BP3 expression vector, the same experiment as performed in *B* showed growth inhibition by OSI-906. (*D*) Wound-healing assay in PaCa-2 cells treated with 1 μM OSI-906 or vehicle. Representative images from experiments repeated in triplicate are shown at the indicated time points. (*E*) Matrigel invasion assay in PaCa-2 cells treated with 1 μM OSI-906 or vehicle. The assay was performed in quadruplicate and is shown as mean ± SD (**$P < 0.01$; two-tailed Student's *t* test). (*F*) Soft-agar colony-formation assay of PaCa-2 cells treated with vehicle or 1 μM OSI-906 for 6 days. Shown are representative images of soft-agar colonies under the microscope at two different magnifications and quantitative analysis of colony formation. The number of colonies of >50 cells was counted under the microscope (*Top*) and using the fluorescence-based CytoSelect Cell Transformation Assay Kit (*Bottom*) (RFU, relative fluorescence units). The assay was performed in quadruplicate and is shown as mean ± SD (***$P < 0.001$, ****$P < 0.0001$; two-tailed Student's *t* test). (Scale bars, 200 μm.) (*G*) Impact of increasing doses of IGF2 supplementation in the culture medium on rescuing cell proliferation. The assay was performed in quadruplicate and is shown as mean ± SD (*$P < 0.05$; two-tailed Student's *t* test; NS, difference not significant). (*H* and *I*) Effects of treatment with OSI-906 on the growth of tumors developed after injection of PaCa-2, Caco-2, or FTC133 cancer cells s.c. into the flanks of nude mice. When the tumor reached ~500 mm^3 volume, mice were treated with either 50 mg/kg OSI-906 or an equal volume of vehicle daily by oral gavage. Data are shown as mean ± SEM. Representative pictures were taken at day 10 of treatment of PaCa-2– and Caco-2–derived tumors and at day 7 of treatment of FTC133-derived tumors. Western blot analysis of xenograft tumor lysates originating from the indicated cells after treatment with vehicle or OSI-906.

prototypic molecular event leading to IGF2BP3 overexpression discovered in this study is a fusion between the *THADA* gene locus on 2p21 and a chromosomal region on 7p15 containing the *LOC389473* gene located upstream of the *IGF2BP3* gene. Chromosomal translocation *t*(2;7) has been previously reported in thyroid tumors leading to the fusion of *THADA* to an untranslated region on chromosome 7, prompting the authors to suggest that its biological effects may involve disrupting the function of THADA, a death receptor-interacting protein (14). Here we show that this chromosomal translocation leads to strong overexpression of the *IGF2BP3* gene located downstream of the fusion point. We were not able to identify *THADA–IGF2BP3* fusion mRNA in the majority of these tumors, and instead observed strong overexpression of the full-length *IGF2BP3* mRNA and protein. Although we cannot exclude that precursor fusion mRNA and protein are made, it appears more likely that IGF2BP3 up-regulation is due to the gene juxtaposition to the *THADA* locus actively transcribed in thyroid cells. Such a mechanism of gene activation, although not common, is known to occur as a consequence of chromosomal rearrangements in other tumor types, particularly in hematological malignancies (5, 15, 16). Our results support the possibility that in virtually all thyroid tumors the fusion on the DNA level occurs upstream of the *IGF2BP3* gene. However, this could not be confirmed directly in this study, because in most tumors the fusions could be studied only at the RNA and not at the DNA sequence level.

IGF2BP3 belongs to the family of IGF2-binding proteins that regulate the expression of IGF2 and other proteins by binding to target mRNAs and controlling their stability and translation (17, 18). It is expressed mostly during embryogenesis and retains no or low expression levels in adult tissues (19, 20). IGF2BP3 has been found to be overexpressed in several cancer types and to affect tumor growth, cell transformation, and metastatic spread (18, 21, 22). However, the mechanisms responsible for IGF2BP3 overexpression in those cancers remain poorly understood, with down-regulation of *let-7* microRNAs proposed as a possible factor (23). Here we show that *THADA–LOC389473* and other *THADA* fusions upstream of the *IGF2BP3* gene represent a previously unknown structural mechanism responsible for *IGF2BP3* overexpression in thyroid and other cancer types.

Thyroid tumors positive for *THADA* fusions demonstrate a distinct phenotype, as they tend to be large in size but fully encapsulated and showing low-grade morphology. In fact, some of these tumors, previously designated papillary carcinomas, may now be reclassified as more indolent, borderline tumors termed NIFTPs (11). However, IGF2BP3 protein overexpression was also observed in a subset of aggressive poorly differentiated thyroid cancers (13). In addition to thyroid tumors, we detected strong IGF2BP3 overexpression by IHC in ∼5 to 15% of other cancer types. Further, we showed that strong overexpression of IGF2BP3 led to posttranscriptional up-regulation of IGF2, activation of IGF1R signaling, and increased cell proliferation, migration, and transformation. Although we cannot exclude that biological effects of IGF2BP3 overexpression may involve not only IGF2 but other mRNA targets, our results provide evidence that IGF2/IGF1R signaling is primarily responsible for biological effects of IGF2BP3 overexpression in these cells.

Our data also suggest that growth of these cells and tumors can be arrested either by blocking IGF2BP3 overexpression or by IGF1R inhibition. This raises the possibility that IGF2BP3 overexpression may serve as a predictor of therapeutic response to IGF1R inhibitors such as OSI-906 (24). Indeed, the IGF1R pathway has been explored as a therapeutic target with either anti-IGF1R antibodies or small-molecule inhibitors. However, most trials showed no clinical benefit of targeting this pathway in patients with advanced cancer (25). In trials that used small-molecule inhibitors, such as OSI-906 (Linsitinib), which binds dually to IGF1R and insulin receptor, clinical response was registered only in a small (1 to 5%) but distinct proportion of patients with solid tumors (24, 26). The results of this study provide early, preclinical evidence that IGF2BP3 overexpression may be used to predict therapeutic response to IGF1R inhibitors in patients with various, frequently highly lethal cancer types, which should be further explored in future studies.

Materials and Methods

Tissue samples were collected and deidentified according to the University of Pittsburgh institutional review board-approved protocol. No patient consent was required. Paired-end whole-genome and whole-exome sequencing was performed on an Illumina HiSeq 2000. Cell-proliferation assays were performed using alamarBlue. Matrigel invasion chambers were used for cell-invasion assays, and soft-agar colony-formation CytoSelect Kits to assess transformation. Detailed methods are provided in *SI Appendix, Materials and Methods*.

ACKNOWLEDGMENTS. We thank the University of Pittsburgh Health Sciences Tissue Bank for providing tissue samples. This work was supported by NIH Grant R01 CA88041 (to Y.E.N.) and by a generous gift from Drs. David and Nancy Brent.

1. Cancer Genome Atlas Research Network (2014) Integrated genomic characterization of papillary thyroid carcinoma. *Cell* 159(3):676–690.
2. Landa I, et al. (2016) Genomic and transcriptomic hallmarks of poorly differentiated and anaplastic thyroid cancers. *J Clin Invest* 126(3):1052–1066.
3. Stransky N, Cerami E, Schalm S, Kim JL, Lengauer C (2014) The landscape of kinase fusions in cancer. *Nat Commun* 5:4846.
4. Carè A, et al. (1986) Translocation of c-myc into the immunoglobulin heavy-chain locus in human acute B-cell leukemia. A molecular analysis. *EMBO J* 5(5):905–911.
5. Aster JC, Longtine JA (2002) Detection of BCL2 rearrangements in follicular lymphoma. *Am J Pathol* 160(3):759–763.
6. Cleary ML, Smith SD, Sklar J (1986) Cloning and structural analysis of cDNAs for bcl-2 and a hybrid bcl-2/immunoglobulin transcript resulting from the t(14;18) translocation. *Cell* 47(1):19–28.
7. Vogelstein B, et al. (2013) Cancer genome landscapes. *Science* 339(6127):1546–1558.
8. LeRoith D, Roberts CT, Jr (2003) The insulin-like growth factor system and cancer. *Cancer Lett* 195(2):127–137.
9. Flanigan SA, et al. (2013) Overcoming IGF1R/IR resistance through inhibition of MEK signaling in colorectal cancer models. *Clin Cancer Res* 19(22):6219–6229.
10. Pollak M (2008) Insulin and insulin-like growth factor signalling in neoplasia. *Nat Rev Cancer* 8(12):915–928.
11. Nikiforov YE, et al. (2016) Nomenclature revision for encapsulated follicular variant of papillary thyroid carcinoma: A paradigm shift to reduce overtreatment of indolent tumors. *JAMA Oncol* 2(8):1023–1029.
12. Scagliotti GV, Novello S (2012) The role of the insulin-like growth factor signaling pathway in non-small cell lung cancer and other solid tumors. *Cancer Treat Rev* 38(4):292–302.
13. Asioli S, et al. (2010) Poorly differentiated carcinoma of the thyroid: Validation of the Turin proposal and analysis of IMP3 expression. *Mod Pathol* 23(9):1269–1278.
14. Drieschner N, et al. (2007) A domain of the thyroid adenoma associated gene (THADA) conserved in vertebrates becomes destroyed by chromosomal rearrangements observed in thyroid adenomas. *Gene* 403(1–2):110–117.
15. Suzukawa K, et al. (1994) Identification of a breakpoint cluster region 3′ of the ribophorin I gene at 3q21 associated with the transcriptional activation of the EVI1 gene in acute myelogenous leukemias with inv(3)(q21q26). *Blood* 84(8):2681–2688.
16. Boxer LM, Dang CV (2001) Translocations involving c-myc and c-myc function. *Oncogene* 20(40):5595–5610.
17. Bell JL, et al. (2013) Insulin-like growth factor 2 mRNA-binding proteins (IGF2BPs): Post-transcriptional drivers of cancer progression? *Cell Mol Life Sci* 70(15):2657–2675.
18. Lederer M, Bley N, Schleifer C, Hüttelmaier S (2014) The role of the oncofetal IGF2 mRNA-binding protein 3 (IGF2BP3) in cancer. *Semin Cancer Biol* 29:3–12.
19. Yisraeli JK (2005) VICKZ proteins: A multi-talented family of regulatory RNA-binding proteins. *Biol Cell* 97(1):87–96.
20. Nielsen J, et al. (1999) A family of insulin-like growth factor II mRNA-binding proteins represses translation in late development. *Mol Cell Biol* 19(2):1262–1270.
21. Lochhead P, et al. (2012) Insulin-like growth factor 2 messenger RNA binding protein 3 (IGF2BP3) is a marker of unfavourable prognosis in colorectal cancer. *Eur J Cancer* 48(18):3405–3413.
22. Hsu KF, et al. (2015) Overexpression of the RNA-binding proteins Lin28B and IGF2BP3 (IMP3) is associated with chemoresistance and poor disease outcome in ovarian cancer. *Br J Cancer* 113(3):414–424.
23. Kugel S, et al. (2016) SIRT6 suppresses pancreatic cancer through control of Lin28b. *Cell* 165(6):1401–1415.
24. Puzanov I, et al. (2015) A phase I study of continuous oral dosing of OSI-906, a dual inhibitor of insulin-like growth factor-1 and insulin receptors, in patients with advanced solid tumors. *Clin Cancer Res* 21(4):701–711.
25. Yee D (2012) Insulin-like growth factor receptor inhibitors: Baby or the bathwater? *J Natl Cancer Inst* 104(13):975–981.
26. Jones RL, et al. (2015) Phase I study of intermittent oral dosing of the insulin-like growth factor-1 and insulin receptors inhibitor OSI-906 in patients with advanced solid tumors. *Clin Cancer Res* 21(4):693–700.